Supplement of The Cryosphere, 16, 3775–3799, 2022
https://doi.org/10.5194/tc-16-3775-2022-supplement

The Cryosphere Open Access EGU

Supplement of

An 11-year record of wintertime snow-surface energy balance and sublimation at 4863 m a.s.l. on the Chhota Shigri Glacier moraine (western Himalaya, India)

Arindan Mandal et al.

Correspondence to: Arindan Mandal (arindan.141@gmail.com)

Table S1. Radiative and turbulent heat fluxes in the High Mountain Asian (HMA) glacier/snow-covered/debris surfaces. All radiative fluxes are in W m^{-2}. R_{net} corresponds to the sum of S_{net} and L_{net}.

	Glacier/Snow-covered site	Region	Period of observation	Lat (°)	Long (°)	Elevation (m)	Surface type	Reference	R_{net} (W m^{-2})	H (W m^{-2})	LE (W m^{-2})
Tibetan Plateau (TP)	Guliya Ice Cap	West Kunlun Mountains, TP	1 Oct 2015 to 30 Sep 2016	81.46	35.26	6000	Ablation zone	Li et al. (2019)	3	12	-11
	Chongce Ice Cap	West Kunlun Mountains, TP	17 Jul to 22 Aug 1987	81.01	35.20	5850	Ablation zone	Takahashi et al. (1989)	44	44	-64
	Urumqi No. 1	Tien Shan, TP	Jun-Aug, 1986-90	86.81	43.12	3840	Ablation zone	Kang and Ohmra (1994)	73	13	-5
	Keqikar Baxi	Southwest Tianshan, TP	16 Jun to 7 Sep 2005	80.09	41.79	4265	Ablation zone	Li et al. (2011)	63	14	-54
	Laohugou No. 12	Western Qilian, TP	1 Jun to 30 Sep, 2010-2015	96.40	39.40	4550	Ablation zone	Sun et al. (2018)	81	8	-13
	Qiyi	Western Qilian, TP	30 Jul to 9 Oct 2011	97.76	39.24	4770	Ablation zone	Wu et al. (2016)	67	28	-21
	Bayi Ice Cap	Qilian Mountains, northern TP	Jun-Sep 2016	98.90	39.01	4800	Ice cap top	Qing et al. (2018)	73	12	-14
	August-one Ice Cap	Qilian Mountains, northern TP	Summer, 2016-2017	98.87	39.02	4820	Ice cap top	Liu et al. (2020) Guo et al. (2018)	61	9	-4
	Parlung No. 4	Southern TP	Annual; 2008-2013	96.92	29.23	4800	Ablation zone	Zhu et al. (2018)	31	11	-21
	Zhadang	Southern TP	Annual; 2008-2013	90.65	30.48	5665	Ablation zone	Zhu et al. (2018)	20	14	-13
	Muztag Ata No. 15	Eastern Pamir, TP	Annual; 2008-2013	75.05	38.23	4400	Ablation zone	Zhu et al. (2018)	8	18	-24
	24 K	Southern TP	Jun to Sep 2016	95.72	29.75	3900	Ablation zone	Yang et al. (2017)	176	-87	-25
	Xiao Dongkemadi	Central TP	7 Oct 1992 to 6 Oct 1993	92.08	33.07	5600	ELA	Liang et al. (2018)	7	12	-6
	Qiangtang No. 1	Inland TP	1 Nov 2012 to 31 Oct 2016	88.70	33.29	5882	Ablation zone	Li et al. (2018)	-7	26	-15
	Guxiang No. 3	South-eastern TP	Jul-Aug, 1965	95.40	29.90	4400	Ablation zone	Wang et al. (1982)	148	63	19
	Xixibangma	South central TP	23 Aug to 11 Sep 1991	85.80	28.45	5700	Ablation zone	Aizen et al. (2002)	28	5	-19
	Muji	Northeastern Pamir, TP	2011-2017	73.74	39.19	4685	Snow/bedrock	Zhu et al. (2020)	25	4	-20
Himalaya	Chhota Shigri	Western Himalaya	8 Jul to 5 Sep 2013	77.51	32.23	4670	Ablation zone	Azam et al. (2014a)	187	31	11
	Dhundi	Western Himalaya	13 Jan to 12 Apr 2005	77.13	32.36	3050	Snow/bedrock	Datt et al. (2008)	83	3	-1
	Ganglass, Ladakh	Western Himalaya	1 Sep 2015 to 31 Aug 2017	77.62	34.25	4727	Permafrost	Wani et al. (2020)	29	14	13
	Ganja La	Central Himalaya	5 March to 25 May 2018	85.56	28.15	4962	Snow cover	Stigter et al. (2021)	42	14	-8
	Yala	Central Himalaya	9 February to 26 May 2018	85.61	28.23	5090	Glacier, snow cover	Stigter et al. (2018) Stigter et al. (2021)	30	25	-25
	Camp II, Everest	Mt. Everest, Central Himalaya	24 Jun to 31 Oct 2019	86.90	27.98	6464	Snow/bedrock	Matthews et al. (2020)	20	3	-8
	South Col, Everest	Mt. Everest, Central Himalaya	22 May to 31 Oct 2019	86.93	27.97	7945	Snow/bedrock	Matthews et al. (2020)	16	11	-25
	AX010	Central Himalaya	25 May to 25 Sep 1978	86.57	27.69	5080	Ablation zone	Kayastha et al. (1999)	55	8	3
	Pindari	Central Himalaya	13 Jun 2016 to 30 Jan 2018	80.01	30.27	3750	Snow/bedrock	Singh et al. (2019)	76	-10	2
	East Rongbuk	Central Himalaya	1 May to 22 July 2005	86.95	28.04	6523	Ablation zone	Liu et al. (2021)	41	12	-20
	Naimona'nyi	Central Himalaya	Oct 2010 to Sept 2018	81.33	30.45	5950	Glacier-wide	Zhu et al. (2021)	8	12	-16

Table S2. The number of days below snow-surface albedo threshold (α_{acc} = 0.4 in this study) in each year and corresponding dates. The data period is DJFMA, 2009-2020.

Year	**No. of days α_{acc} < 0.4**	**α_{acc} < 0.4 dates**
2009/10	-	-
2010/11	-	-
2011/12	16	1-6 Dec, 18 Dec, 22-23 Dec, 26-31 Dec (2011), 1 Jan 2012
2012/13	-	-
2013/14	9	1-2 Dec, 4-5 Dec, 16-19 Dec (2013), 3 Jan 2014
2014/15	1	11 Dec 2014
2015/16	-	-
2016/17	30	1-24 Dec, 30 Dec (2016), 16-20 Apr 2017
2017/18	18	13-23 Jan, 1-5 Feb, 29-30 Apr (2018)
2018/19	-	-
2019/20	-	-
Total	**74**	-

Table S3. Monthly mean and range of observed meteorological and SEB variables at the AWS-M for DJFMA, 2009-2020. Precipitation records from the glacier base camp are between 12 July 2012 and 30 April 2018.

Variable	Dec	Jan	Feb	Mar	Apr	Min.	Max.	Mean
Meteorology								
T_{air} (°C)	-13.0	-15.5	-14.2	-11.0	-6.9	**-21.9**	**0.1**	**-12.1**
T_s (°C)	-16.2	-17.7	-15.1	-11.9	-7.5	**-27.4**	**0.6**	**-13.7**
RH (%)	32	41	49	45	49	**10**	**99**	**43**
q ($g\ kg^{-1}$)	0.8	0.8	1.1	1.3	2.0	**0.2**	**4.3**	**1.2**
u ($m\ s^{-1}$)	5.3	5.4	6.0	4.6	3.7	**0.7**	**15.9**	**5.0**
S_{TOA} ($W\ m^{-2}$)	212	226	261	301	343	**211**	**447**	**303**
S_{in} ($W\ m^{-2}$)	124	135	165	236	293	**28**	**414**	**191**
S_{out} ($W\ m^{-2}$)	70	82	107	158	197	**21**	**286**	**123**
L_{in} ($W\ m^{-2}$)	181	191	208	213	226	**123**	**290**	**204**
L_{out} ($W\ m^{-2}$)	249	243	253	266	285	**207**	**319**	**260**
α_{acc} [§]	0.59	0.63	0.68	0.69	0.69	**0.22**	**0.94**	**0.66**
CF [§]	0.46	0.46	0.47	0.36	0.33	**0.06**	**0.99**	**0.41**
P (mm)	56	109	135	150	119	-	-	**569** [Y]
P (%) [+]	10	19	24	26	21	-	-	**100**
SEB								
S_{net} ($W\ m^{-2}$)	54	52	58	78	97	**4**	**207**	**68**
L_{net} ($W\ m^{-2}$)	-68	-52	-45	-54	-58	**-129**	**18**	**-55**
R_{net} ($W\ m^{-2}$)	-11	2	15	26	41	**-50**	**124**	**15**
H ($W\ m^{-2}$)	8	1	-6	-12	-12	**-118**	**102**	**-4**
LE ($W\ m^{-2}$)	-35	-30	-37	-42	-47	**-145**	**0**	**-38**
H+LE ($W\ m^{-2}$)	-27	-29	-42	-49	-54	**-204**	**73**	**-40**
F ($W\ m^{-2}$)	-38	-27	-28	-28	-18	**-151**	**127**	**-28**

[§]Mean values between 09:00 and 16:00 IST and values are rounded to 2 decimal places.
[Y]Sum of DJFMA precipitation (see Fig. 4).
[+]Sum of DJFMA monthly values.

Table S4. Mean yearly values of DJFMA for observed meteorological and SEB variables during 2009-2020 at the AWS-M.

Variable	2009/10	2010/11	2011/12	2012/13	2013/14	2014/15	2015/16	2016/17	2017/18	2018/19	2019/20	Mean
Meteorology												
T_{air} (°C)	-11.1	-12.5	-13.4	-12	-12.9	-11.6	-11.7	-11.9	-10.7	-12.5	-12.4	**-12.1**
T_s (°C)	-16.1	-15	-13.6	-13.9	-14	-13.1	-12.9	-12.3	-11.9	-14.3	-12.5	**-13.7**
RH (%)	45	43	49	41	45	41	41	48	41	45	42	**43**
q ($g\ kg^{-1}$)	1.4	1.1	1.3	1.2	1.1	1.2	1.2	1.4	1.3	1.2	1.2	**1.2**
u ($m\ s^{-1}$)	4.9	5.2	5.7	4.7	5.3	4.8	4.9	5.4	4.7	5.0	4.5	**5.0**
S_{in} ($W\ m^{-2}$)	161	195	192	195	192	194	199	193	200	197	200	**192**
L_{in} ($W\ m^{-2}$)	-	196	208	200	205	203	203	213	205	207	206	**204**
α_{acc}[§]	0.72	0.66	0.63	0.63	0.64	0.64	0.63	0.65	0.62	0.76	0.65	**0.66**
CF[§]	0.49	0.39	0.43	0.40	0.44	0.40	0.37	0.44	0.39	0.41	0.39	**0.41**
SEB												
S_{net} ($W\ m^{-2}$)	47	68	72	74	69	73	75	72	78	54	71	**68**
L_{net} ($W\ m^{-2}$)	-	-56	-50	-58	-53	-58	-59	-51	-61	-49	-57	**-55**
R_{net} ($W\ m^{-2}$)		11	22	16	17	15	16	22	17	5	14	**15**
H ($W\ m^{-2}$)	13	-4	-16	-6	-13	-3	1	-10	-5	1	-9	**-4**
LE ($W\ m^{-2}$)	-17	-34	-43	-39	-43	-40	-40	-43	-48	-30	-43	**-38**
F ($W\ m^{-2}$)	-	-26	-48	-39	-49	-42	-36	-45	-49	-25	-53	**-40**

[§]Mean values between 09:00 and 16:00 IST and values are rounded to 2 decimal places.

Table S5. Interannual correlation coefficient (*r;* n = 11) between cumulative sublimation (S_c) and primary meteorological variables for 2009-2020. '*' refers to $p < 0.05$.

	***RH* > 80%**	T_s	T_{air}	***u***	***RH***	S_{in}	L_{in}	α_{acc}	*CF*
S_c	-0.76*	0.85*	-0.15	-0.10	-0.50	0.79*	0.03	-0.78*	-0.69*

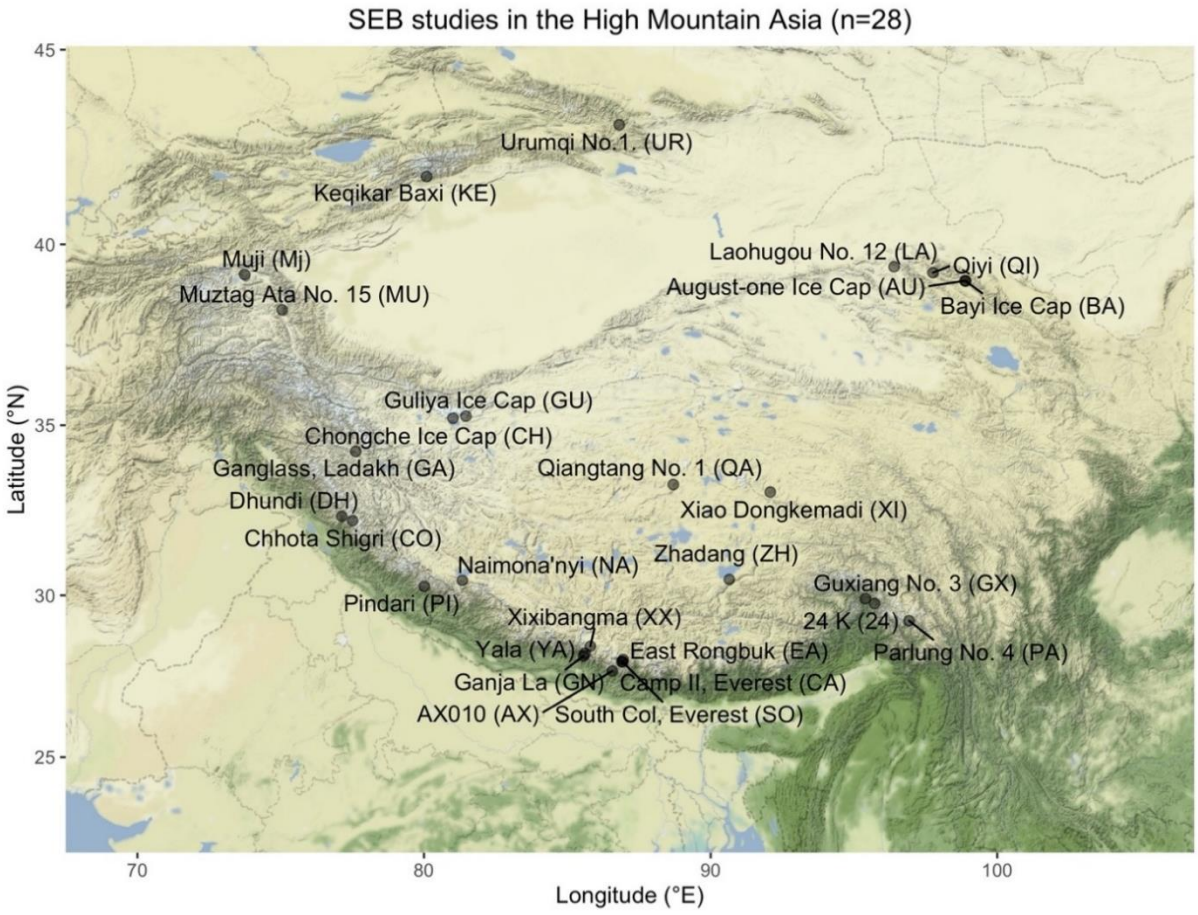

Fig. S1. Location of the existing glacier/snow-cover SEB sites across HMA (listed in Table S1). The background is the Stamen terrain map. The figure is generated using the 'ggmap' package (Kahle and Wickham, 2013) in the R environment.

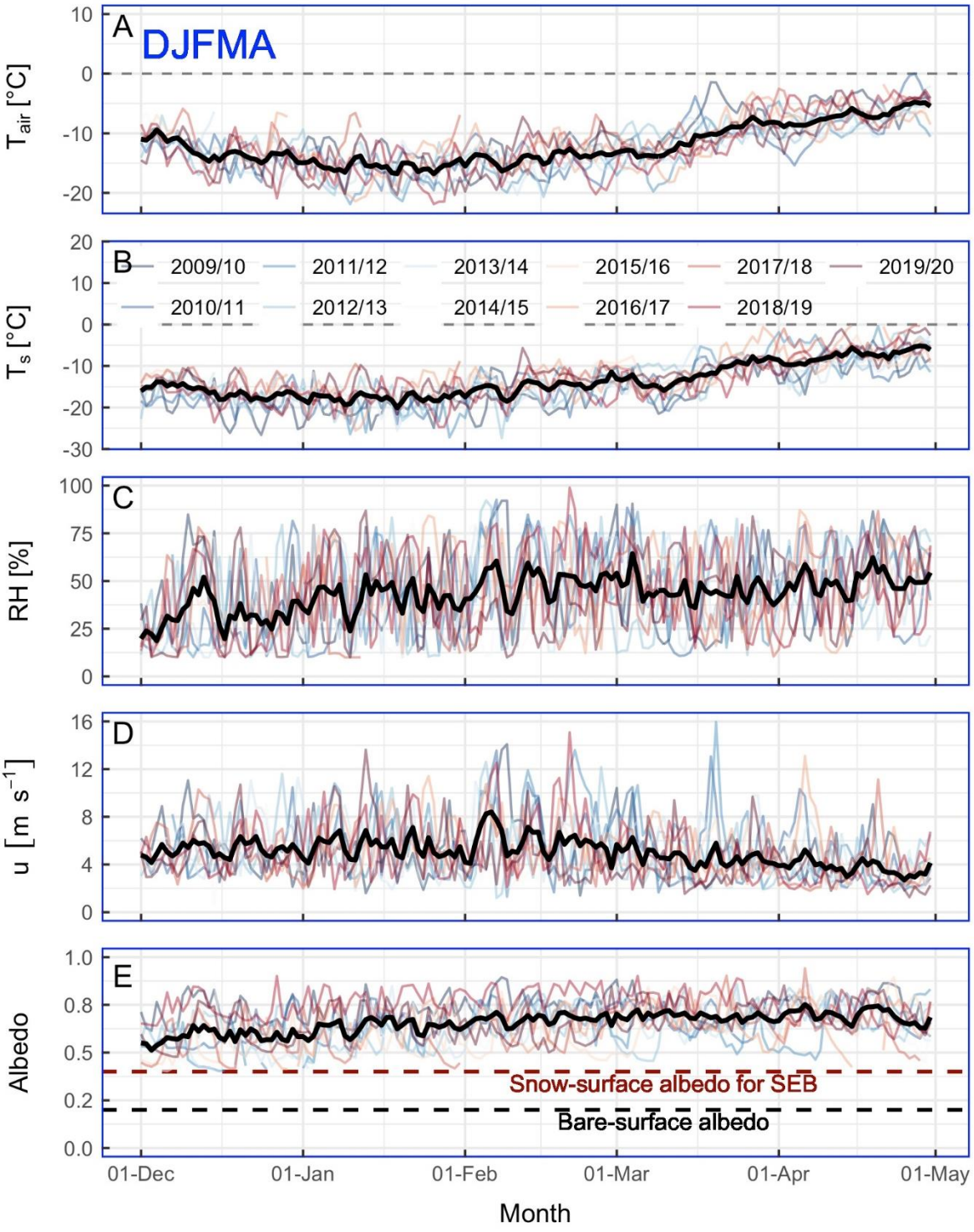

Fig. S2. Daily averages (1 December to 30 April) of half-hourly measurements of air (T_{air}) and surface temperature (T_s), relative humidity (RH), wind speed (u) and surface albedo (α_{acc}) at the AWS-M for 2009-2020. Snow-surface albedo (α_{acc} = 0.4) for SEB analysis and bare-surface albedo (α_{acc} = 0.2) are also shown in the albedo panel (E). The bold black line in the daily panel highlights the mean of all years.

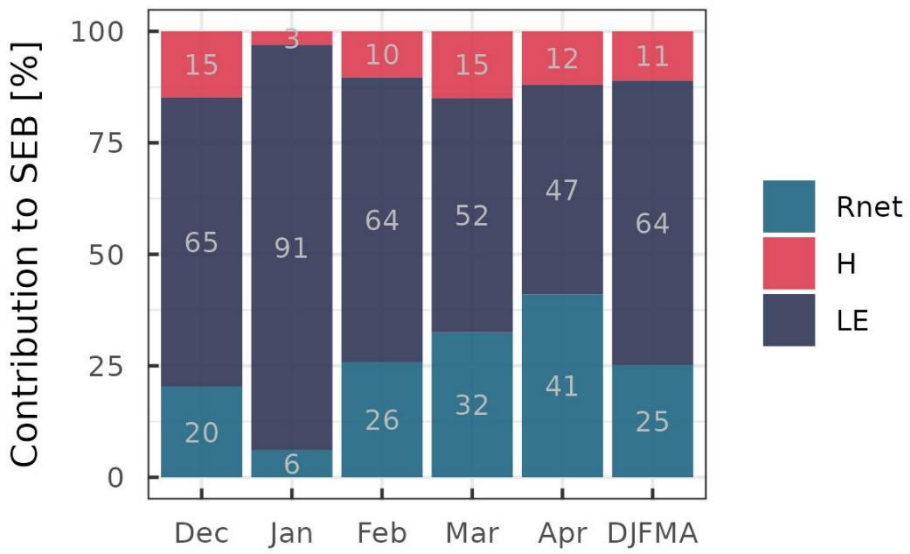

Fig. S3. Monthly proportional contribution of R_{net}, H and LE to SEB. DJFMA is the mean of all months. The proportional contributions were calculated by following the approach of Zhang et al. (2013).

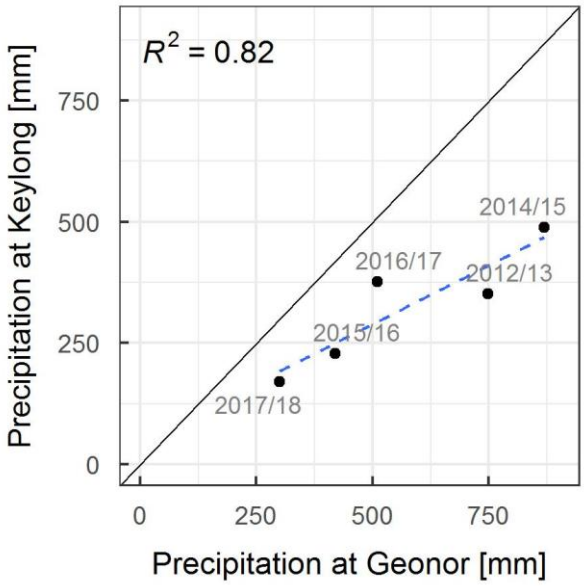

Fig. S4. Comparison of DJFMA precipitation recorded at the Geonor/base camp station (3850 m a.s.l.) and IMD's Keylong station (3119 m a.s.l.). Both stations are ~60 km away. Keylong data is taken from: https://weathershimla.nic.in/en-IN/climatedata.html. DJFMA precipitation is the sum of records between December and April of each hydrological year. Five years data are available for Geonor; years are shown on top of the respective data points. Also shown is the 1:1 line. This figure illustrates the correlation between Keylong (original) and Geonor precipitation (R^2 = 0.82); however, the RMSE is 274 mm. A precipitation gradient of 0.1 m km^{-1} was applied following Azam et al. (2014b) to extrapolate Keylong's precipitation to the AWS-M altitude. The extrapolated precipitation showed better agreement to measured, with RMSE reduced to 139 mm.

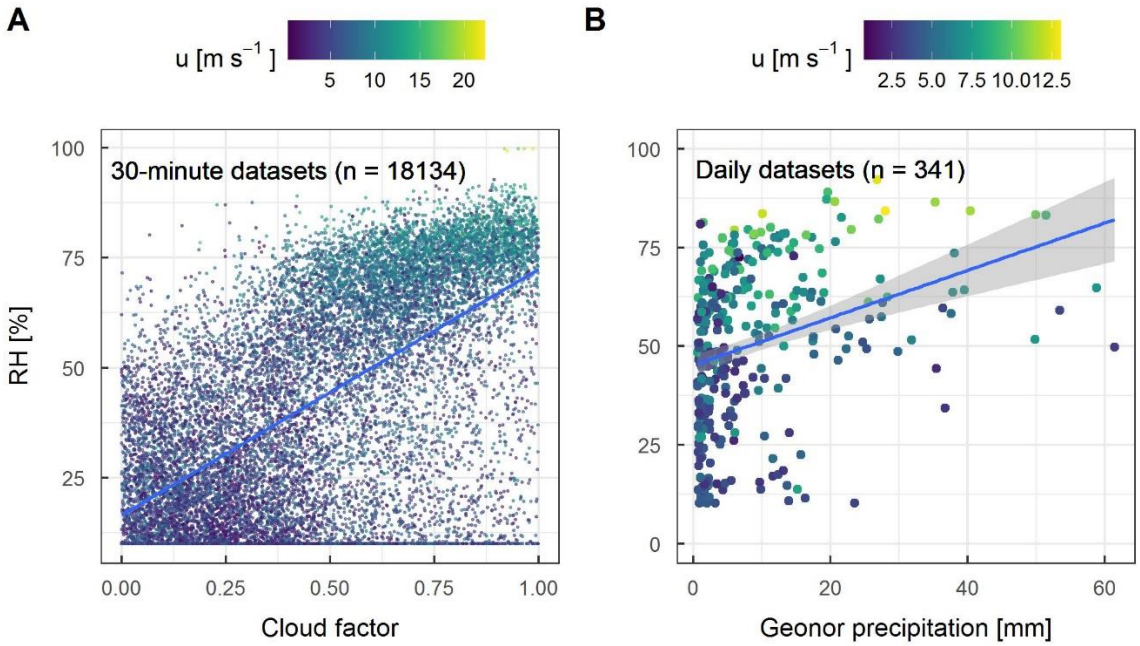

Fig. S5. (A) Relationship between relative humidity, wind speed and cloud factor, and (B) relative humidity, cloud factor and precipitation. The number of data points is mentioned on the respective panel. Precipitation was recorded at the glacier base camp at 3850 m a.s.l.

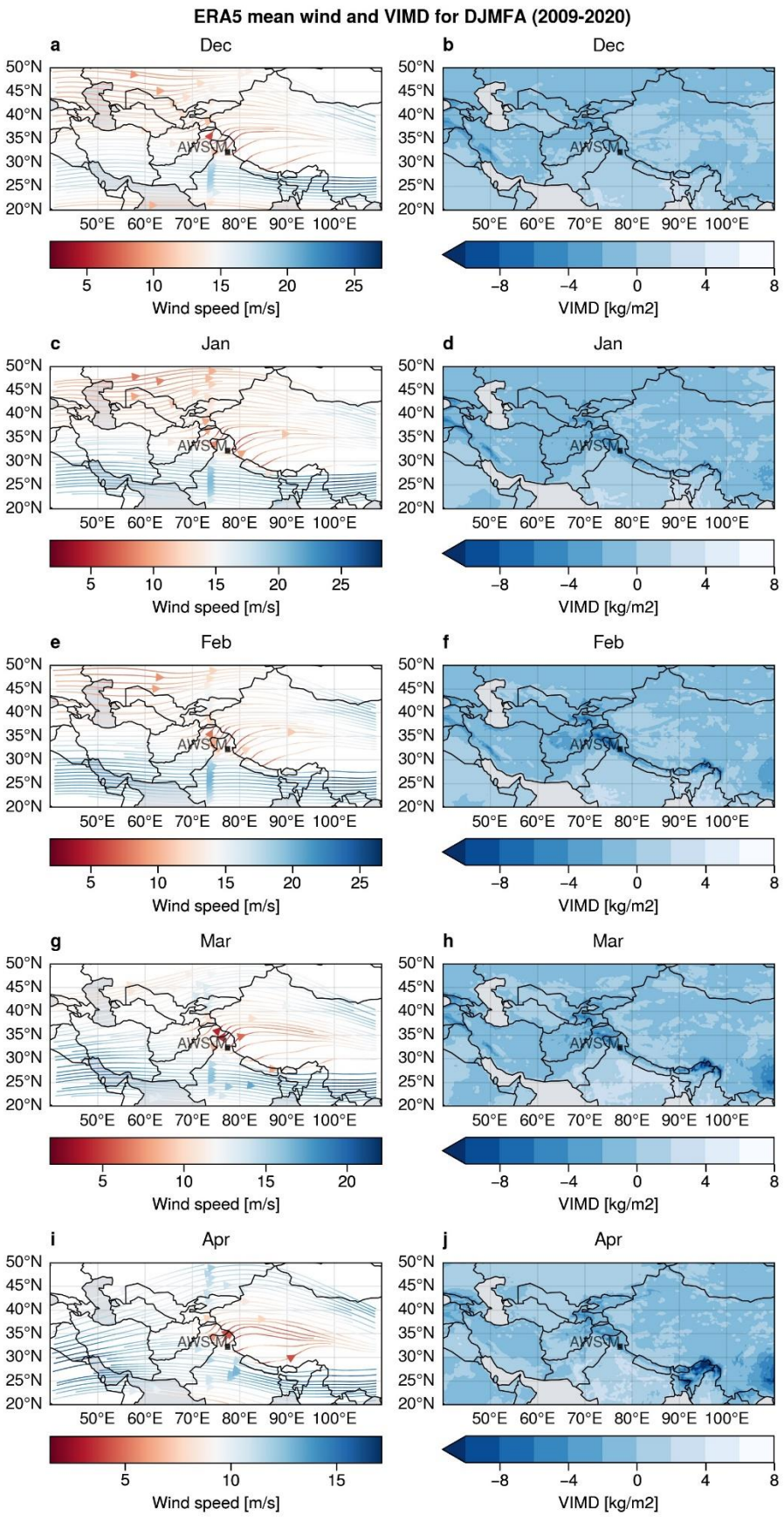
ERA5 mean wind and VIMD for DJMFA (2009-2020)
a
Dec
b
Dec
c
Jan
d
Jan
e
Feb
f
Feb
g
Mar
h
Mar
i
Apr
j
Apr
AWSM
50°N
45°N
40°N
35°N
30°N
25°N
20°N
50°E 60°E 70°E 80°E 90°E 100°E
5 10 15 20 25
Wind speed [m/s]
−8 −4 0 4 8
VIMD [kg/m2]

Fig. S6: Mean horizontal wind (from *u* and *v* components) and vertically integrated moisture divergence (VIMD) at 500 hPa for DJFMA during 2009-2020 based on ERA5 data. ERA5 data was downloaded from the Climate Data Store, ECMWF (https://cds.climate.copernicus.eu). AWS-M location is shown with black square and text. Arrows in the wind plots refer to the direction of winds. Plots are generated in Python using several packages, mainly xarray, proplot, matplotlib. Plot template was taken from Lalande et al. (2021). Note: the higher negative values (dark blue areas) of VIMD (i.e., large moisture convergence) refers to precipitation intensification in a particular region (https://apps.ecmwf.int/codes/grib/param-db/?id=213).

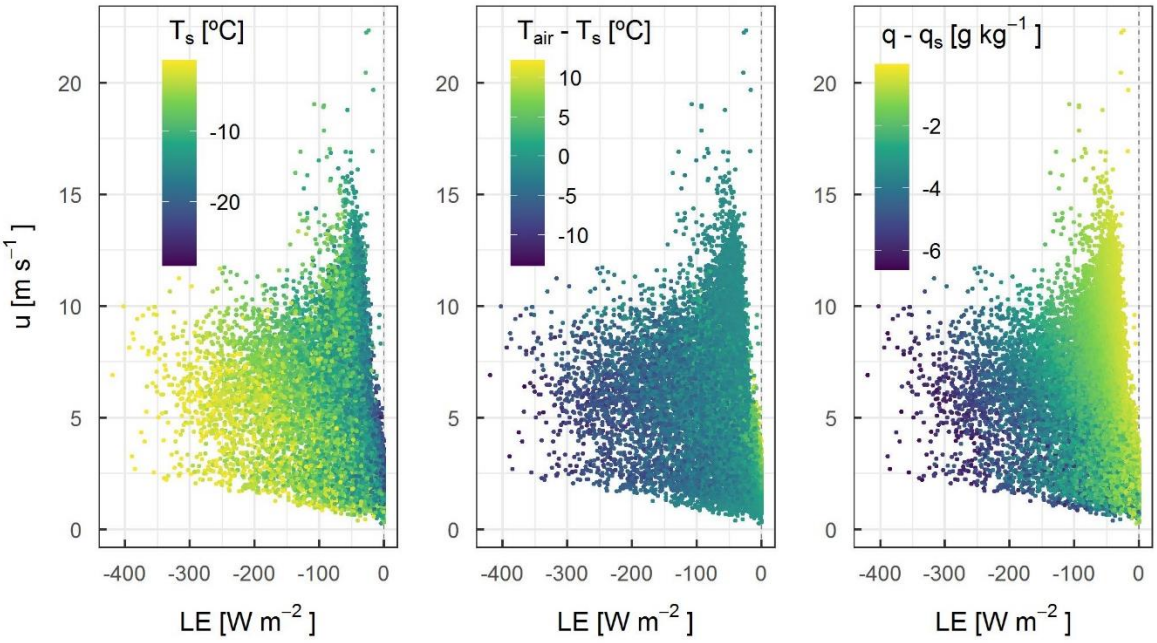

Fig. S7. Relationship of *LE* with *u*, T_s, T_{air}-T_s and q-q_s over the study period for DJFMA, 2009-2020. The half-hourly data points are used (n = 13217) between 09:00 and 16:00 IST.

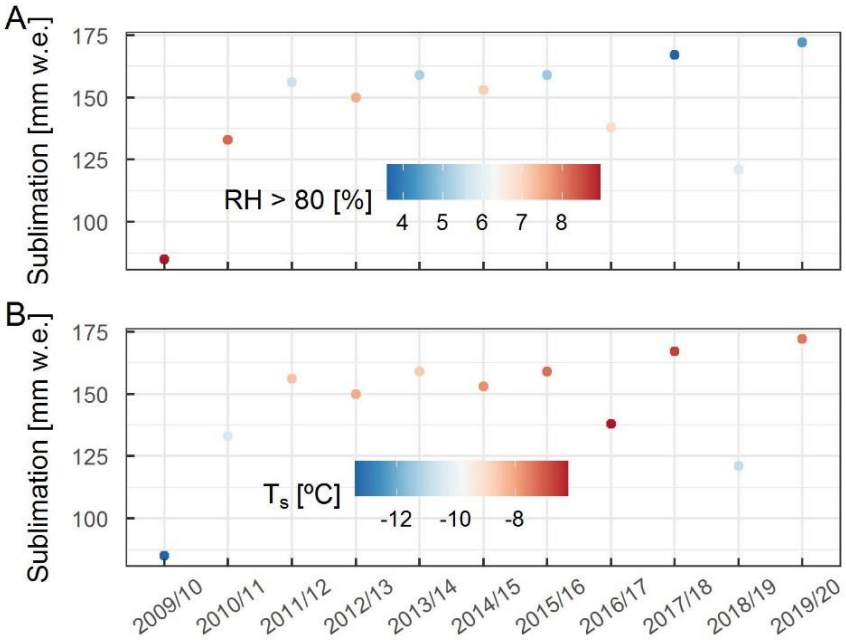

Fig. S8. Relationship between cumulative sublimation and $RH > 80\%$ and T_s at the AWS-M for DJFMA, 2009-2020. *RH* and T_s are for the daytime between 08:00 and 16:00 IST.

References

Aizen, V. B., Aizen, E. M., and Nikitin, S. A.: Glacier regime on the northern slope of the Himalaya (Xixibangma glaciers), Quaternary International, 97–98, 27–39, https://doi.org/10.1016/S1040-6182(02)00049-6, 2002.

Azam, M. F., Wagnon, P., Vincent, C., Ramanathan, A. L., Favier, V., Mandal, A., and Pottakkal, J. G.: Processes governing the mass balance of Chhota Shigri Glacier (western Himalaya, India) assessed by point-scale surface energy balance measurements, The Cryosphere, 8, 2195–2217, https://doi.org/10.5194/tc-8-2195-2014, 2014a.

Azam, M. F., Wagnon, P., Vincent, C., Ramanathan, A., Linda, A., and Singh, V. B.: Reconstruction of the annual mass balance of Chhota Shigri glacier, Western Himalaya, India, since 1969, Ann. Glaciol., 55, 69–80, https://doi.org/10.3189/2014AoG66A104, 2014b.

Datt, P., Srivastava, P. K., Negi, P. S., and Satyawali, P. K.: Surface energy balance of seasonal snow cover for snow-melt estimation in N-W Himalaya, J Earth Syst Sci, 117, 567–573, https://doi.org/10.1007/s12040-008-0053-7, 2008.

Guo, S., Chen, R., Liu, G., Han, C., Song, Y., Liu, J., Yang, Y., Liu, Z., Wang, X., Liu, X., Wang, L., and Zheng, Q.: Simple Parameterization of Aerodynamic Roughness Lengths and the

Turbulent Heat Fluxes at the Top of Midlatitude August-One Glacier, Qilian Mountains, China, Journal of Geophysical Research: Atmospheres, 123, 12,066-12,080, https://doi.org/10.1029/2018JD028875, 2018.

Jing, L., Liu, ShiYin., Zhang, Yong., Shangguan, D.: Surface energy balance of Keqicar Glacier, Tianshan Mountains, China, during ablation period, Sci. Cold Arid Regi, 3:197-205, 2011.

Kahle, D., Wickham, H.: ggmap: Spatial Visualization with ggplot2, The R Journal, 5(1):144-161, 2013.

Kang, E., Ohmura, A.: A parameterized energy balance model of glacier melting on the Tianshan Mountain, Acta Geograph Sin, 49:467–476, 1994.

Kayastha, R. B., Ohata, T., and Ageta, Y.: Application of a mass-balance model to a Himalayan glacier, Journal of Glaciology, 45, 559–567, https://doi.org/10.3189/S002214300000143X, 1999.

Lalande, M., Ménégoz, M., Krinner, G., Naegeli, K., and Wunderle, S.: Climate change in the High Mountain Asia in CMIP6, Earth Syst. Dynam., 12, 1061–1098, https://doi.org/10.5194/esd-12-1061-2021, 2021.

Li, S., Yao, T., Yang, W., Yu, W., and Zhu, M.: Glacier Energy and Mass Balance in the Inland Tibetan Plateau: Seasonal and Interannual Variability in Relation to Atmospheric Changes, Journal of Geophysical Research: Atmospheres, 123, 6390–6409, https://doi.org/10.1029/2017JD028120, 2018.

Li, S., Yao, T., Yu, W., Yang, W., and Zhu, M.: Energy and mass balance characteristics of the Guliya ice cap in the West Kunlun Mountains, Tibetan Plateau, Cold Regions Science and Technology, 159, 71–85, https://doi.org/10.1016/j.coldregions.2018.12.001, 2019.

Liang, L., Cuo, L., and Liu, Q.: The energy and mass balance of a continental glacier: Dongkemadi Glacier in central Tibetan Plateau, Sci Rep, 8, 12788, https://doi.org/10.1038/s41598-018-31228-5, 2018.

Liu, W., Zhang, D., Qin, X., Broeke, M. R. van den, Jiang, Y., Yang, D., and Ding, M.: Monsoon Clouds Control the Summer Surface Energy Balance on East Rongbuk glacier (6523 m above sea level), the northern of Mt. Qomolangma (Everest), Journal of Geophysical Research: Atmospheres, https://doi.org/10.1029/2020JD033998, 2021.

Liu, Y., Hou, S., Wang, Y., and Song, L.: Distribution of borehole temperature at four high-altitude alpine glaciers in Central Asia, J. Mt. Sci., 6, 221–227, https://doi.org/10.1007/s11629-009-0254-9, 2009.

Matthews, T., Perry, L. B., Koch, I., Aryal, D., Khadka, A., Shrestha, D., Abernathy, K., Elmore, A. C., Seimon, A., Tait, A., Elvin, S., Tuladhar, S., Baidya, S. K., Potocki, M., Birkel, S. D., Kang, S., Sherpa, T. C., Gajurel, A., and Mayewski, P. A.: Going to Extremes: Installing the World's Highest Weather Stations on Mount Everest, Bulletin of the

American Meteorological Society, 101, E1870–E1890, https://doi.org/10.1175/BAMS-D-19-0198.1, 2020.

Qing, W., Han, C., and Liu, J.: Surface energy balance of Bayi Ice Cap in the middle of Qilian Mountains, China, J. Mt. Sci., 15, 1229–1240, https://doi.org/10.1007/s11629-017-4654-y, 2018.

Singh, N., Singhal, M., Chhikara, S., Karakoti, I., Chauhan, P., and Dobhal, D. P.: Radiation and energy balance dynamics over a rapidly receding glacier in the central Himalaya, International Journal of Climatology, 40, 400–420, https://doi.org/10.1002/joc.6218, 2020.

Stigter, E. E., Litt, M., Steiner, J. F., Bonekamp, P. N. J., Shea, J. M., Bierkens, M. F. P., and Immerzeel, W. W.: The Importance of Snow Sublimation on a Himalayan Glacier, Front. Earth Sci., 6, https://doi.org/10.3389/feart.2018.00108, 2018.

Stigter, E. E., Steiner, J. F., Koch, I., Saloranta, T. M., Kirkham, J. D., and Immerzeel, W. W.: Energy and mass balance dynamics of the seasonal snowpack at two high-altitude sites in the Himalaya, Cold Regions Science and Technology, 183, 103233, https://doi.org/10.1016/j.coldregions.2021.103233, 2021.

Sun, W., Qin, X., Wang, Y., Chen, J., Du, W., Zhang, T., and Huai, B.: The response of surface mass and energy balance of a continental glacier to climate variability, western Qilian Mountains, China, Climate Dynamics, 50, 3557–3570, https://doi.org/10.1007/s00382-017-3823-6, 2018.

Takahashi, S., Ohata, T., Xie, Y.: Characteristics of heat and water fluxes on glacier and ground surfaces in the West Kunlun Mountains, Bull. Glacier Res., 7, 1989.

Wang, Z., Deng, Y., Zeng, X.: Water-heat conditions for maritime glaciers developing in Guxiang, Tibetan Region, In Memoirs of Lanzhou Institute of Glaciology and Geocryology, CAS, No. 3. Science Press, Beijing, 82–90, 1982.

Wani, J. M., Thayyen, R. J., Ojha, C. S. P., and Gruber, S.: The surface energy balance in a cold and arid permafrost environment, Ladakh, Himalayas, India, The Cryosphere, 15, 2273–2293, https://doi.org/10.5194/tc-15-2273-2021, 2021.

Wu, X., He, J., Jiang, X., and Wang, N.: Analysis of surface energy and mass balance in the accumulation zone of Qiyi Glacier, Tibetan Plateau in an ablation season, Environ Earth Sci, 75, 785, https://doi.org/10.1007/s12665-016-5591-8, 2016.

Yang, W., Yao, T., Zhu, M., and Wang, Y.: Comparison of the meteorology and surface energy fluxes of debris-free and debris-covered glaciers in the southeastern Tibetan Plateau, Journal of Glaciology, 63, 1090–1104, https://doi.org/10.1017/jog.2017.77, 2017.

Zhang, G., Kang, S., Fujita, K., Huintjes, E., Xu, J., Yamazaki, T., Haginoya, S., Wei, Y., Scherer, D., Schneider, C., and Yao, T.: Energy and mass balance of Zhadang glacier surface, central Tibetan Plateau, J. Glaciol., 59, 137–148, https://doi.org/10.3189/2013JoG12J152, 2013.

Zhu, M., Yang, W., Yao, T., Tian, L., Thompson, L. G., and Zhao, H.: The Influence of Key Climate Variables on Mass Balance of Naimona'nyi Glacier on a North-Facing Slope in the Western Himalayas, Geophys Res Atmos, 126, https://doi.org/10.1029/2020JD033956, 2021.

Zhu, M., Yao, T., Xie, Y., Xu, B., Yang, W., and Yang, S.: Mass balance of Muji Glacier, northeastern Pamir, and its controlling climate factors, Journal of Hydrology, 590, 125447, https://doi.org/10.1016/j.jhydrol.2020.125447, 2020.

Zhu, M., Yao, T., Yang, W., Xu, B., Wu, G., Wang, X., and Xie, Y.: Reconstruction of the mass balance of Muztag Ata No. 15 glacier, eastern Pamir, and its climatic drivers, Journal of Glaciology, 1–16, https://doi.org/10.1017/jog.2018.16, 2018.